Sandwich nanohybrid of single-walled carbon nanohorns–TiO_2–porphyrin for electrocatalysis and amperometric biosensing towards chloramphenicol†

Wenwen Tu, Jianping Lei,* Lin Ding and Huangxian Ju*

Received (in Cambridge, UK) 6th April 2009, Accepted 14th May 2009
First published as an Advance Article on the web 9th June 2009
DOI: 10.1039/b906876g

A sandwich nanohybrid of single-walled carbon nanohorn–TiO_2–porphyrin was prepared *via* the dentate binding of TiO_2 nanoparticles to carboxylate groups, which showed an excellent electrocatalytic activity towards the reduction of chloramphenicol in neutral media, leading to a highly sensitive and stable amperometric biosensor for chloramphenicol.

Single-walled carbon nanohorns (SWNHs), as a dahlia-flower-like spherical superstructure of aggregated nanosized graphitic tubes, have attracted considerable attention for hydrogen storage and drug delivery due to the high surface area, excellent porosity, and considerable internal nanospace.[1] The functionalization of SWNHs can improve the solubilization for applications in a variety of fields. Especially, SWNHs functionalized with porphyrins, a mimic of enzymes, is a promising biomaterial for photoinduced electron and energy transfer, and fluorescence properties.[2]

Meanwhile, the photovoltaic, photophysical, photocatalytic properties of porphyrin bound TiO_2 nanoparticles have been widely studied.[3] The porphyrin bound carboxylic groups can spontaneously adsorb onto TiO_2 nanoparticles by bridging, ester-like or bidentate binding.[3b,c] This work uses hydroxyferriprotoporphyrin as a model and TiO_2 nanoparticles as a bridge to prepare a sandwich nanohybrid of SWNHs–TiO_2–porphyrin as shown in Fig. 1. The resulting nanohybrid shows excellent electrocatalysis toward reduction of chloramphenicol (CAP), leading to a sensitive amperometric biosensor for CAP.

CAP is a bacteriostatic antibiotic for the treatment of life threatening infections such as childhood meningitis and typhoid fever. Owing to serious side effects such as aplastic anemia, leucopenia and thrombocytopenia, many countries and organizations have imposed a strict ban on the use of CAP in food-producing animals.[4] Therefore, effective monitoring of CAP is urgently important. Several methods such as surface plasmon resonance,[5a] liquid chromatography electrospray ionization tandem mass spectrometry[5b] and immunochip processes[5c] have been developed for determination of CAP. Although the detection limits of some methods reach down to fM or nM levels, they require expensive equipment, time-consuming derivatization and extraction, and professional operation. Particularly, it is difficult to use these methods for *in situ* or online monitoring. This work provides a low-cost method for convenient detection of CAP. Compared with those based on amperometric biosensors[6] this method shows higher sensitivity and a wider concentration range.

X-Ray photoelectron spectra (XPS) of O 1s were recorded to characterize the formation of the sandwich nanohybrid. The O 1s XPS spectrum of the porphyrin consisted of two peaks assigned to carbon–oxygen double bonding (C=O, 532.3 eV) and single bonding (C–O, 533.7 eV) (Fig. S1a in ESI†). By contrast, the O 1s XPS spectrum of TiO_2–porphyrin exhibited three chemically different peaks corresponding to Ti–O at 531.1 eV, C=O at 532.7 eV and C–O at 533.9 eV (Fig. 2(a)). These results indicated that oxygen of the carboxylate groups of the porphyrin bound to the TiO_2 surface.[3c] Compared with the O 1s peak at 529.85 eV for Ti–O of TiO_2,[7a] the Ti–O bond in TiO_2–porphyrin showed higher energy due to the presence of the electron-donating carboxylate groups of the porphyrin.[7b] The Ti–O bond in SWNHs–TiO_2–porphyrin showed a binding energy of 530.3 eV, lower than that in TiO_2–porphyrin (Fig. 2(b)) due to the relatively lower amount of carboxylate bound to TiO_2 surface. The intensities of C=O at 532.0 eV and C–O at 533.2 eV for SWNHs–TiO_2–porphyrin were slightly larger due to the presence of COO groups on

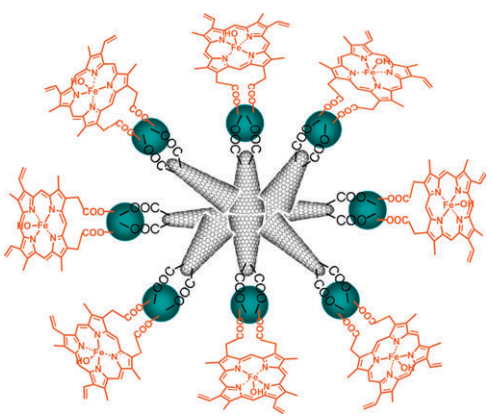

Fig. 1 Schematic illustration of the structure of SWNHs–TiO_2–porphyrin nanohybrids. Other oxygenated species (*i.e.*, hydroxyls, carbonyls, carboxyls, *etc.*) introduced during the oxidation of SWNHs are not shown for simplicity.

Key Laboratory of Analytical Chemistry for Life Science (Education Ministry of China), Department of Chemistry, Nanjing University, Nanjing 210093, P. R. China. E-mail: jpl@nju.edu.cn, hxju@nju.edu.cn; Fax: +86-25-83593593; Tel: +86-25-83593593

† Electronic supplementary information (ESI) available: Related reagents, instrumentation, praparation of nanohybrid and modified electrode, XPS, IR Raman spectra and TEM images, electrochemical behaviors of SWNHs–TiO_2–porphyrin modified GCE, chemical structures, effects of SWNHs and TiO_2 contents on electrocatalysis. See DOI: 10.1039/b906876g

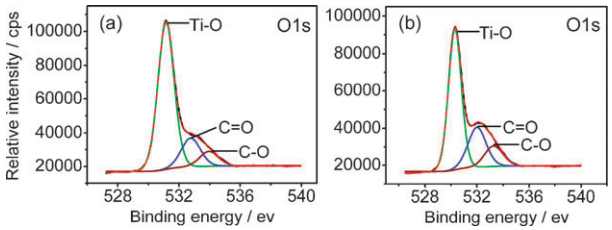

Fig. 2 O 1s XPS spectra of TiO_2–porphyrin (a) and SWNHs–TiO_2–porphyrin (b).

SWNHs produced by the oxidation treatment (Fig. S1b in ESI†).[1b] These changes identified that a sandwich nanohybrid of SWNHs–TiO_2–porphyrin was formed *via* the dentate binding of TiO_2 nanoparticles to the carboxylate groups of the porphyrin and to SWNHs.

The FTIR spectrum of the porphyrin showed a peak assigned to the C═O stretch mode of carboxylic group at 1722 cm^{-1} and a peak attributed to the B_{3u} vibration of porphyrin at 1378 cm^{-1} (Fig. S2A in ESI†).[8] The appearance of the peaks at 1730, 1581 and 1205 cm^{-1} for SWNHs indicated the presence of carboxylic and carboxylate oxygen-containing groups on the SWNHs surface (Fig. S2B in ESI†). Compared with SWNHs, the small shifts of carboxylic groups of SWNHs–TiO_2 resulted from the dentate binding between the carboxylic group of SWNHs and TiO_2 (Fig. S2C in ESI†), indicating a good electronic communication between SWNHs and TiO_2. In addition, the fingerprint region of porphyrin appeared from 1200 to 700 cm^{-1} in SWNHs–TiO_2–porphyrin (Fig. S2D in ESI†), suggesting that porphyrin had successfully assembled on SWNHs–TiO_2.

The Raman spectrum of SWNHs showed a disorder-induced D-band at 1344 cm^{-1} and a tangential stretch G-band at 1573 cm^{-1} (Fig. S3B in ESI†). Comparing with SWNHs, these bands of SWNHs–TiO_2 were slightly shifted to 1350 and 1578 cm^{-1} with remarkably enhanced strength, respectively (Fig. S3C in ESI†), which should contribute to the TiO_2-to-SWNHs charge transfer mechanism related to the surface state energy levels of the TiO_2 semiconductor.[9] Moreover, the ratios of D- to G-bands for SWNHs and SWNHs–TiO_2 were 1.15 and 1.13, respectively, which indicated the functionalization of SWNHs with TiO_2 did not damage the structure of the SWNHs. TEM images of SWNHs and SWNHs–TiO_2–porphyrin films further demonstrated that the TiO_2 stacked on the surface of SWNHs and the original dahlia-flower-like morphology of the SWNH aggregates was still sustained (Fig. S4 in ESI†). The average diameter of the SWNHs was estimated to be around 80 nm, which was consistent with the previous report.[2b]

By using the $Fe(CN)_6^{3-/4-}$ redox couple as a probe, Nyquist plots were used to monitor the modification of electrodes (Fig. S5(a) in ESI†). The bare GCE showed an electron transfer resistance of about 360 Ω, while the coating of porphyrin on the electrode increased dramatically the resistance to about 960 Ω, suggesting that porphyrin film blocked the electron exchange between the redox probe and electrode surface. However, the porphyrin-TiO_2 modified GCE showed an electron transfer resistance of 822 Ω, indicating the presence of TiO_2 could improve the electron transfer. Compared with

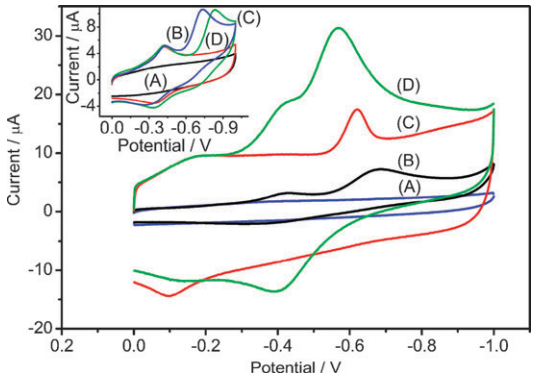

Fig. 3 Cyclic voltammograms of bare GCE (A), TiO_2–porphyrin (B), SWNHs–TiO_2 (C), SWNHs–TiO_2–porphyrin (D) modified GCEs in 0.1 M pH 7.0 PBS with 100 μM CAP at 100 mV s^{-1}. Inset: cyclic voltammograms of IL (A), porphyrin-IL (B) modified GCEs in 0.1 M pH 7.0 PBS containing 100 μM CAP, and porphyrin-IL modified GCE in 0.1 M pH 7.0 PBS in the presence (C) and absence (D) of 100 μM *p*-nitrophenol at 100 mV s^{-1}.

both porphyrin and porphyrin-TiO_2 modified GCEs, the electron transfer resistance of SWNHs–TiO_2–porphyrin was 318 Ω, implying the SWNHs further accelerated the electron transfer due to the excellent electronic conductivity. In addition, SWNHs–TiO_2–porphyrin modified GCEs showed a pair of redox peaks (Fig. S5(b) in ESI†), and the electrode reaction showed a surface controlled electrode process (Fig. S6 in ESI†), which could be attributed to the redox couple of Fe^{III}/Fe^{II} in the immobilized porphyrin.

Upon addition of CAP in PBS the cyclic voltammogram showed another cathodic peak with current of 4.3 and 7.9 μA at −0.68 and −0.62 V at TiO_2–porphyrin and SWNHs–TiO_2 modified GCEs, respectively, while the bare electrode did not show any response (Fig. 3). The presence of SWNHs accelerated the electronic reduction of CAP. At SWNHs–TiO_2–porphyrin modified GCE the reduction peak of CAP further increased to 22.0 μA and the peak potential positively moved to −0.56 V, showing a synergic effect due to the superstructure of the nanohybrid material. Here TiO_2 nanoparticles acted as bridges to form the sandwich nanohybrid, SWNHs increased the electron transfer rate of the sensing layer, and porphyrin acted as a catalyst to reduce the reduction potential of CAP by the 'mediated mechanism'.[3f] The reduction potential was much more positive than those with amperometric biosensors,[6] producing an excellent amperometric biosensing application for CAP detection.

In order to confirm the catalytic behavior of porphyrins in electrocatalyzing the reduction of CAP, ionic liquid was used as a solvent to dissolve the porphyrin for its immobilization on an electrode surface. Comparing curves A, B and D in the inset in Fig. 3, the porphyrin undoubtedly acted as a catalyst to electrocatalyze the reduction of CAP. Further, dichloroacetic acid and *p*-nitrophenol (Fig. S7 in ESI†) were used to mimic the dichloroacetic group and nitroaromatic group of CAP, respectively, to identify the reduction site of CAP. Upon addition of 100 μM dichloroacetic acid in PBS, no response was observed at IL-porphyrin modified GCEs, indicating the reduction site was not the dichloroacetic group. In contrast, when adding 100 μM *p*-nitrophenol in PBS, the same

electrocatalytic appearance as the reduction of CAP could be observed (curve C, inset in Fig. 3), thus the electroactive site was the nitroaromatic group. To our best knowledge, this is the first report that porphyrins can be used as catalysts for CAP reduction.

At optimal contents of SWNHs and TiO_2 nanoparticles for preparation of SWNHs–TiO_2–porphyrin nanohybrids (Fig. S8 in ESI†), the current–time curve of SWNHs–TiO_2–porphyrin modified GCE upon successive addition of CAP at an applied potential of −0.56 V clearly illustrated that the modified GCE could respond very rapidly to the change in the CAP concentration within only 5 s (Fig. S9 in ESI†). The linear detection range could be up to 135.7 μM with a detection limit of 0.9 nM at a signal to noise ratio of 3, which was much lower than those of 5.0 nM at IL-gold nanoparticles-SWNTs modified GCE,[6c] 47 nM at a carbon fibre microelectrode[6a] and 420 nM at a Nafion coated screen-printed electrode.[6b] The linear range of five orders of magnitude was much wider than those reported above. Thus the SWNHs–TiO_2–porphyrin based biosensor for CAP showed a better performance.

The CAP biosensor also showed good fabrication reproducibility with a relative standard deviation of only 4.6% as estimated from the slopes of the calibration plots at five freshly prepared SWNHs–TiO_2–porphyrin modified GCEs prepared at different electrodes. The coefficients of variation of the current signals for seven repeated injections of 5 nM and 5 μM CAP examined at the same modified electrode were 4.3 and 3.9%, respectively, indicating a good operational reproducibility. Consecutive cyclic voltammetric sweeps also showed acceptable stability of the sensor (Fig. S10 in ESI†). When the biosensor was not in use, it was stored in the shade at room temperature. No obvious decrease in the amperometric response to CAP was observed after 5 days of storage and it retained 91.7% of initial amperometric response after 25 days. This implied that the structure of the SWNHs/porphyrin-TiO_2 film was very efficient for retaining the activity of porphyrin and preventing it from leaking out of the biosensor.

The effects of common interfering species on the biosensor response were examined in a biological sample. For example, ions (Na^+, K^+, Mg^{2+}, Cu^{2+}, Ca^{2+}, Zn^{2+}, NH_4^+, Cl^-, SO_4^{2-}, PO_4^{3-}), saccharide (sucrose, glucose), and antibiotic (chlorotetracycline, streptomycin, penicillin) at 1000 times concentration of CAP did not interfere with the amperometric response of CAP. These results indicated that the amperometric biosensor had an excellent specificity in the detection of CAP.

The concentration of CAP in injection was detected with the proposed biosensor to be 0.40 ± 0.017 M (5 measurements) without any need of sample pretreatment except an appropriate dilution of sample. This value was close to 0.39 M according to the instruction of CAP injection detected by high performance liquid chromatography. Furthermore, recovery testing was carried out to demonstrate the validity of the proposed method. After 15 nM and 5 μM of CAP were added to this sample, the obtained recoveries of CAP were 105.4 ± 4.3% and 96.7 ± 3.9%, respectively, indicating acceptable accuracy.

In summary, a sandwich nanohybrid of SWNHs–TiO_2–porphyrin is prepared *via* the dentate binding of the carboxylate groups onto TiO_2 nanoparticles as bridges for highly sensitive amperometric biosensing of CAP. The direct electrochemistry corresponding to the redox couple of Fe^{III}/Fe^{II} of the porphyrin is realized. The SWNHs–TiO_2–porphyrin modified electrode shows excellent electrocatalytic activity toward reduction of CAP due to the synergic effect among SWNHs, TiO_2 and porphyrin. The electroactive site of CAP is confirmed to be the nitroaromatic group. The designed biosensor exhibited good analytical performance in the detection of CAP such as rapid response, wide linear range, low detection limit, good fabrication reproducibility, and acceptable accuracy. The sandwich nanostructure of SWNHs–TiO_2–porphyrin provides a functional electrocatalyst to construct a sensitive biosensor and can be extended for the application in the photovoltaic- and photo-catalysis in solar cells.

This work was supported by the fund for Creative Research Groups (20821063), Major Research Plan (90713015), Key (20535010, 20835006) and General (20875044, 20745003, 20705012) Programs from NSFC, PhD Fund for Young Teachers (20070284052) and Science Foundation of Jiangsu (BK2007570).

Notes and references

1 (*a*) G. Rotas, A. S. D. Sandanayaka, N. Tagmatarchis, T. Ichihashi, M. Yudasaka, S. Iijima and O. Ito, *J. Am. Chem. Soc.*, 2008, **130**, 4725; (*b*) S. Utsumi, H. Honda, Y. Hattori, H. Kanoh, K. Takahashi, H. Sakai, M. Abe, M. Yudasaka, S. Iijima and K. Kaneko, *J. Phys. Chem. C*, 2007, **111**, 5572.

2 (*a*) C. Cioffi, S. Campidelli, C. Sooambar, M. Marcaccio, G. Marcolongo, M. Meneghetti, D. Paolucci, F. Paolucci, C. Ehli, G. M. A. Rahman, V. Sgobba, D. M. Guldi and M. Prato, *J. Am. Chem. Soc.*, 2007, **129**, 3938; (*b*) G. Pagona, A. S. D. Sandanayaka, Y. Araki, J. Fan, N. Tagmatarchis, M. Yudasaka, S. Iijima and O. Ito, *J. Phys. Chem. B*, 2006, **110**, 20729.

3 (*a*) A. J. Mozer, P. Wagner, D. L. Officer, G. G. Wallace, W. M. Campbell, M. Miyashita, K. Sunahara and S. Mori, *Chem. Commun.*, 2008, 4741; (*b*) J. Rochford, D. Chu, A. Hagfeldt and E. Galoppini, *J. Am. Chem. Soc.*, 2007, **129**, 4655; (*c*) S. Eu, S. Hayashi, T. Umeyama, A. Oguro, M. Kawasaki, N. Kadota, Y. Matano and H. Imahori, *J. Phys. Chem. C*, 2007, **111**, 3528; (*d*) S. O. Obare, T. Ito and G. J. Meyer, *J. Am. Chem. Soc.*, 2006, **128**, 712; (*e*) J. R. Stromberg, J. D. Wnuk, R. A. F. Pinlac and G. J. Meyer, *Nano Lett.*, 2006, **6**, 1284; (*f*) T. Ito and G. J. Meyer, *Environ. Eng. Sci.*, 2007, **24**, 31.

4 (*a*) R. Sheridan, B. Policastro, S. Thomas and D. Rice, *J. Agric. Food Chem.*, 2008, **56**, 3509; (*b*) Council Regulation (EEC) 1430/94 of 22 June 1994, *Off. J. Eur. Commun.* L156, 1994, 6.

5 (*a*) J. Yuan, R. Oliver, M. I. Aguilar and Y. Q. Wu, *Anal. Chem.*, 2008, **80**, 8329; (*b*) R. Mohamed, J. Richoz-Payot, E. Gremaud, P. Mottier, E. Yilmaz, J. C. Tabet and P. A. Guy, *Anal. Chem.*, 2007, **79**, 9557; (*c*) Z. X. Gao, N. Liu, Q. L. Cao, L. Zhang, S. Q. Wang, W. Yao and F. H. Chao, *Biosens. Bioelectron.*, 2009, **24**, 1445.

6 (*a*) L. Agüí, A. Guzmán, P. Yáñez-Sedeño and J. M. Pingarrón, *Anal. Chim. Acta*, 2002, **461**, 65; (*b*) J. C. Chen, J. L. Shih, C. H. Liu, M. Y. Kuo and J. M. Zen, *Anal. Chem.*, 2006, **78**, 3752; (*c*) F. Xiao, F. Q. Zhao, J. W. Li, R. Yan, J. J. Yu and B. Z. Zeng, *Anal. Chim. Acta*, 2007, **596**, 79.

7 (*a*) D. M. Chen, D. Yang, J. Q. Geng, J. H. Zhu and Z. Y. Jiang, *Appl. Surf. Sci.*, 2008, **255**, 2879; (*b*) H. J. Shin, S. M. Kim, S. M. Yoon, A. Benayad, K. K. Kim, S. J. Kim, H. K. Park, J. Y. Choi and Y. H. Lee, *J. Am. Chem. Soc.*, 2008, **130**, 2062.

8 X. X. Zhang, Y. X. Zhang and J. Z. Jiang, *Spectrochim. Acta, Part A*, 2005, **61**, 2576.

9 L. B. Yang, X. Jiang, W. D. Ruan, B. Zhao, W. Q. Xu and J. R. Lombardi, *J. Phys. Chem. C*, 2008, **112**, 20095.

Electronic Supplementary Information (ESI) for Chemical Communications

Sandwich nanohybrid of single-walled carbon nanohorns-TiO_2-porphyrin for electrocatalysis and amperometric biosensing toward chloramphenicol

Wenwen Tu, Jianping Lei,* Lin Ding and Huangxian Ju*

Key Laboratory of Analytical Chemistry for Life Science (Education Ministry of China),

Department of Chemistry, Nanjing University, Nanjing 210093, P.R. China

Experimental

Materials. Hydroxyferriprotoporphyrin (hematin, 98%) and chloramphenicol (99%) were purchased from Alfa Aesar China Ltd. (China). Single-walled carbon nanohorns (SWNHs) were kindly provided from Professor Sumio Iijima leading carbon nanotube project in Japan Science and Technology Agency. TiO_2 nanopowder (anatase, <25 nm, 99.7%) was purchased from Aldrich (USA). All other chemicals were of analytical grade. Aqueous solutions were prepared with twice-distilled water. 0.1 M phosphate buffer solution (PBS) was always employed as supporting electrolyte deaerated with high purity nitrogen. The pH value of PBS was 7.0 except those indicated.

Apparatus. X-ray photoelectron spectroscopic (XPS) measurements were performed with an ESCALAB 250 spectrometer (Thermo-VG Scientific, USA) with ultra-high vacuum generators. Transmission electron micrographs (TEM) were obtained using a JEM-2100 TEM (JEOL, Japan). Fourier-transform infrared spectra (FTIR) were obtained on a NEXUS 870 FTIR instrument (Nicolet, USA). Resonance

Raman spectra were recorded on a Renishaw-inVia Raman microscope (Renishaw, United Kingdom). Electrochemical impedance spectroscopic (EIS) measurements were carried out on a PGSTAT30/FRA2 system (Autolab, Netherlands) in 0.1 M KCl solution containing 5 mM $K_3[Fe(CN)_6]$/5 mM $K_4[Fe(CN)_6]$. The impedance spectra were recorded in the frequency range of 10^{-2}–10^5 Hz. The amplitude of the applied sine wave potential in each case was 5 mV. Cyclic voltammetric experiments were performed on a CHI 610C electrochemical workstation (CH Instruments Inc., USA), and amperometric experiments were preformed on a CHI 812B electrochemical workstation (CH Instruments Inc., USA). All experiments were carried out at room temperature using a conventional three-electrode system with a modified glassy carbon electrode (GCE) as working, a platinum wire as auxiliary and a saturated calomel electrode as reference electrodes.

Preparation of SWNHs-TiO_2-porphyrin and modified GCEs. SWNHs were dispersed in 30% HNO_3 and then refluxed for 24 h at 140 °C to obtain carboxylic group functionalized SWNHs. The resulting suspension was centrifuged, and the sediment was washed with twice-distilled water until the pH reached 6.0. The oxidized SWNHs were dispersed in twice-distilled water to form a stable suspension with concentration of 2 mg mL^{-1}. Hydroxyferriprotoporphyrin was dissolved in 5 mL dimethyl sulphoxide (DMSO) to get a DMSO solution of 20 mM porphyrin. 100 mg TiO_2 nanoparticles were ultrasonically dispersed in 5mL twice-distilled water to get a suspension of 20 mg ml^{-1} TiO_2. Then, 5 ml DMSO solution of 20 mM porphyrin was added into 5 ml suspension of 20 mg ml^{-1} TiO_2 with the aid of ultrasonic agitation to obtain a suspension of TiO_2-porphyrin, following with discarding the upper solution to remove free porphyrin. Further, 2 ml suspension of 2 mg ml^{-1} SWNHs was added into 2 ml suspension of 10 mg ml^{-1} TiO_2-porphyrin with the aid of ultrasonic agitation to produce a suspension of SWNHs-TiO_2-porphyrin. After discarding the upper solution, the resulting sediment was dispersed in water to obtain SWNHs-TiO_2-porphyrin suspension with concentration of 6 mg ml^{-1}.

The GCEs (3 mm in diameter) were polished to a mirror finish with 1.0 and 0.05 μm alumina slurry on chamois leathers, and then washed ultrasonically in absolute ethanol and twice-distilled water for two minutes respectively, dried at room temperature. Then 10 μL suspension of 6 mg ml^{-1} SWNHs-TiO_2-

porphyrin was dropped on the GCE and dried at room temperature to obtain the SWNHs-TiO_2-porphyrin modified electrode. Similarly, TiO_2-porphyrin, SWNHs-TiO_2 and the modified GCEs were prepared in the absence of SWNHs and porphyrin, respectively.

O1s X-ray photoelectron spectra of porphyrin and SWNHs

The XPS characterization was performed to analyze the composition of porphyrin and SWNHs. The O1s XPS spectrum of porphyrin consists of two peaks assigned to carbon-oxygen double bonding (C=O, 532.3 eV) and single bonding (C-O, 533.7 eV) (Fig. S1a). These peaks could be produced by the oxidation treatment of SWNHs (C=O at 532.0 eV and C-O at 533.6 eV) (Fig. S1b).

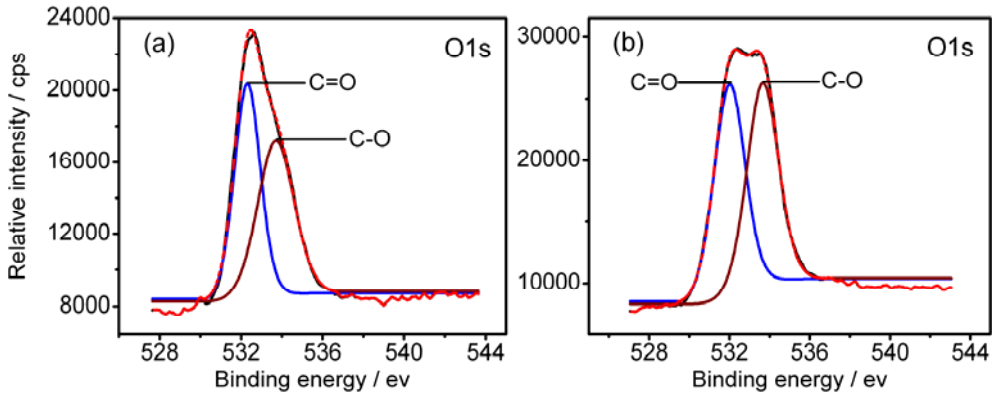

Fig. S1. O1s XPS spectra of porphyrin (a) and SWNHs (b).

FTIR spectra

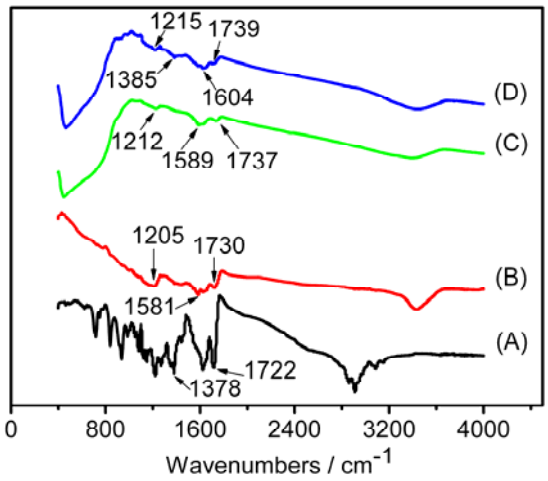

Fig. S2 FTIR spectra of porphyrin (A), SWNHs (B), SWNHs-TiO_2 (C), and SWNHs-TiO_2-porphyrin (D)**.**

Raman spectra

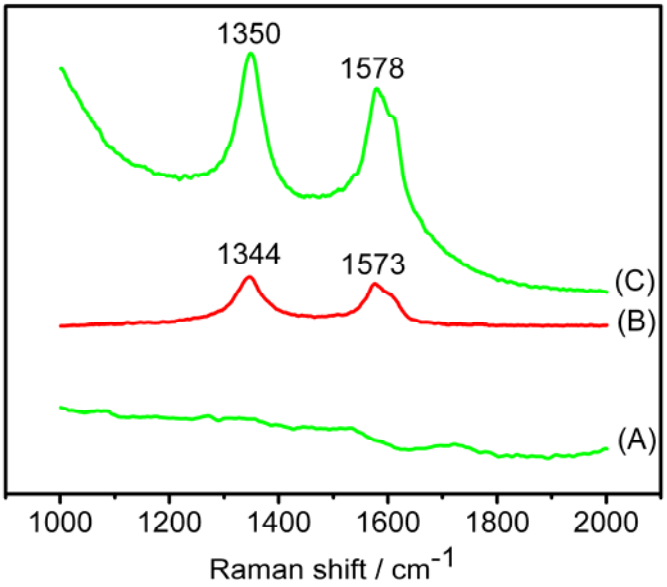

Fig. S3 Raman spectra of TiO_2 (A), SWNHs (B), and SWNHs-TiO_2 (C).

TEM characterization

The formation of SWNHs-TiO_2-porphyrin was further examined by transmission electron micrographs (TEM). The TEM images of SWNHs and SWNHs-TiO_2-porphyrin films demonstrated that TiO_2 stacked on the surface of SWNHs and the original dahlia-flower-like morphology of the SWNH aggregates was still sustained (Fig. S4). The average diameter of the flower like-hybrid material was estimated to be around 80 nm.

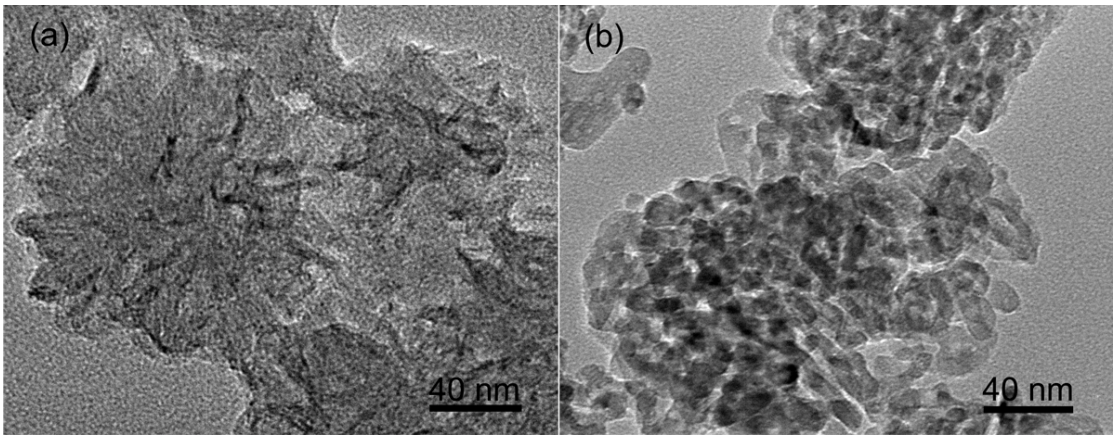

Fig. S4 TEM of SWNHs (a) and SWNHs-TiO_2-porphyrin (b).

Electrochemical behaviors of SWNHs-TiO_2-porphyrin modified GCE

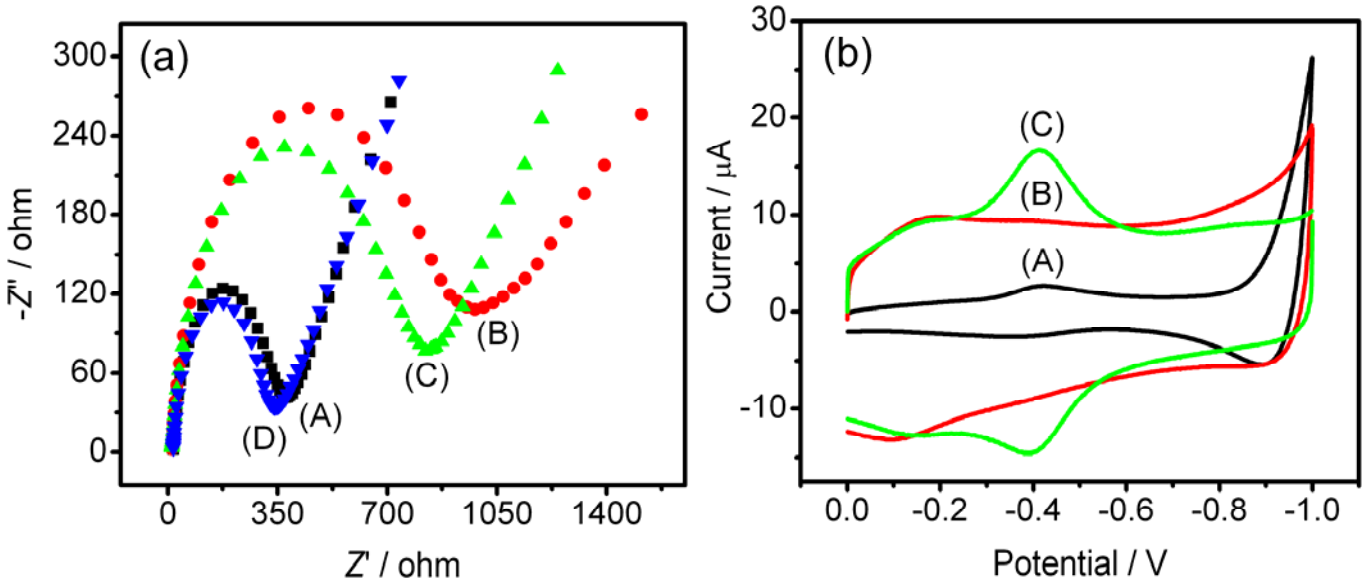

Fig. S5 Electrochemical impedance spectra of bare (A), porphyrin (B), TiO_2-porphyrin (C), SWNHs-TiO_2-porphyrin (D) modified GCEs in 0.1 M KCl solution containing 5 mM $K_3[Fe(CN)_6]$/5 mM $K_4[Fe(CN)_6]$ (a) and cyclic voltammograms of TiO_2-porphyrin (A), SWNHs-TiO_2 (B), SWNHs-TiO_2-porphyrin (C) modified GCEs in 0.1 M pH 7.0 PBS at 100 mV s^{-1} (b).

The reduction and oxidation peak currents of SWNHs-TiO_2-porphyrin modified GCE increased linearly with the scan rate in the range of 40–500 mV s^{-1} (Fig. S6), while the difference of redox peak potentials showed slight increase, indicating a surface controlled electrode process. The redox peak potentials of porphyrin in the film showed strong dependence on the pH value of the external solution. With the increasing pH from 5 to 9, the formal potential, midpoint of reduction and oxidation potentials, exhibited a linear relationship with a slope of –48.9 mV pH^{-1}.

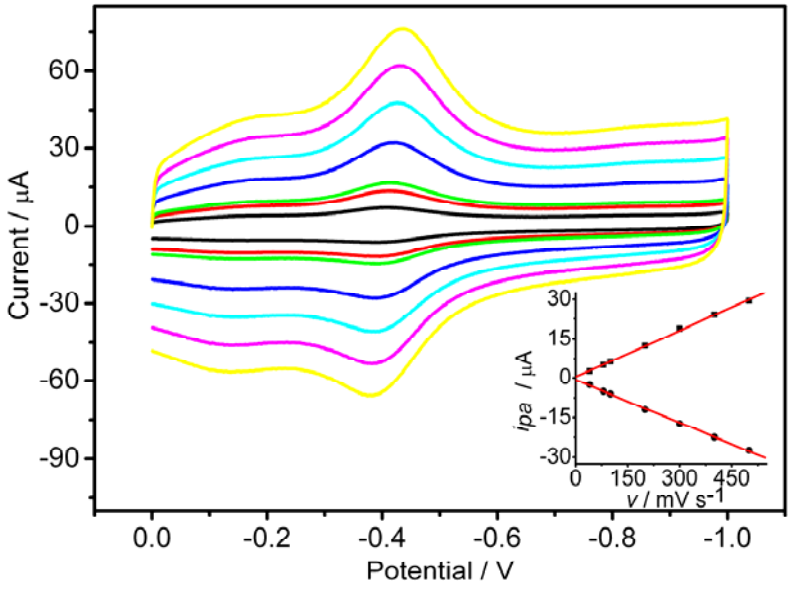

Fig. S6 Cyclic voltammograms of SWNHs-TiO_2-porphyrin modified GCE at 40, 80, 100, 200, 300, 400 and 500 mV s^{-1} (from inner to outer) in 0.1 M pH 7.0 PBS. Inset: plots of oxidation and reduction peak currents vs. *v*.

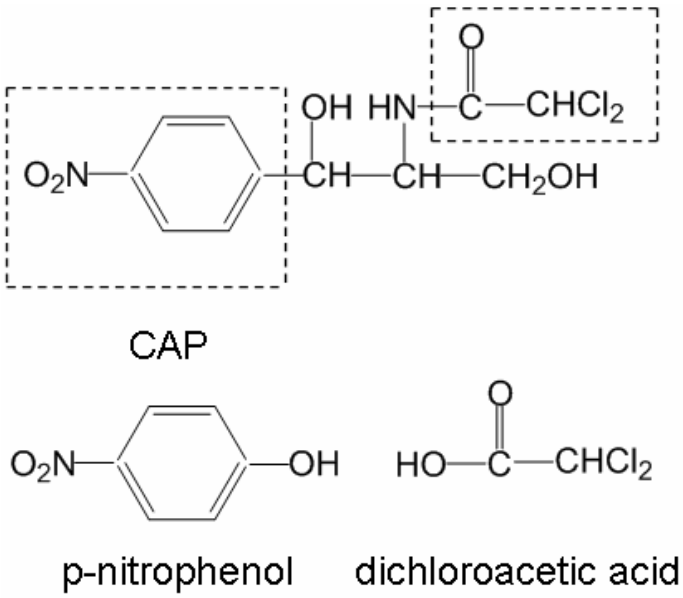

Fig. S7 Chemical structures of CAP, p-nitrophenol and dichloroacetic acid.

Effects of SWNHs and TiO_2 contents for preparation of SWNHs-TiO_2-porphyrin on electrocatalytic peak current

In Fig. S8(a), with the increasing SWNHs content the electrocatalytic current increased and then trended to a constant value, which was attributed to the excellent electric conductivity of SWNHs for accelerating the electron transfer between porphyrin and GCE and the electrocatalysis toward reduction of CAP. The saturation of SWNHs in the nanohybrid resulted in the plateau. Thus 1 mg mL^{-1} SWNHs was chosen for the preparation of SWNHs-TiO2-porphyrin nanohybrid.

TiO_2 content was also an important parameter for obtaining an optimal electrocatalytic response. As shown in Fig. S8(b), with the increasing TiO_2 content, the electrocatalytic current of CAP increased and reached a maximum value at 5 mg ml^{-1}. However, when the TiO_2 content was more than 10 mg ml^{-1}, the electrocatalytic current decreased because excessive TiO_2 nanoparticles slowed down the electron transfer in the elelctrocatalytic process. This work used 5 mg mL^{-1} TiO_2 for the preparation of the nanohybrid.

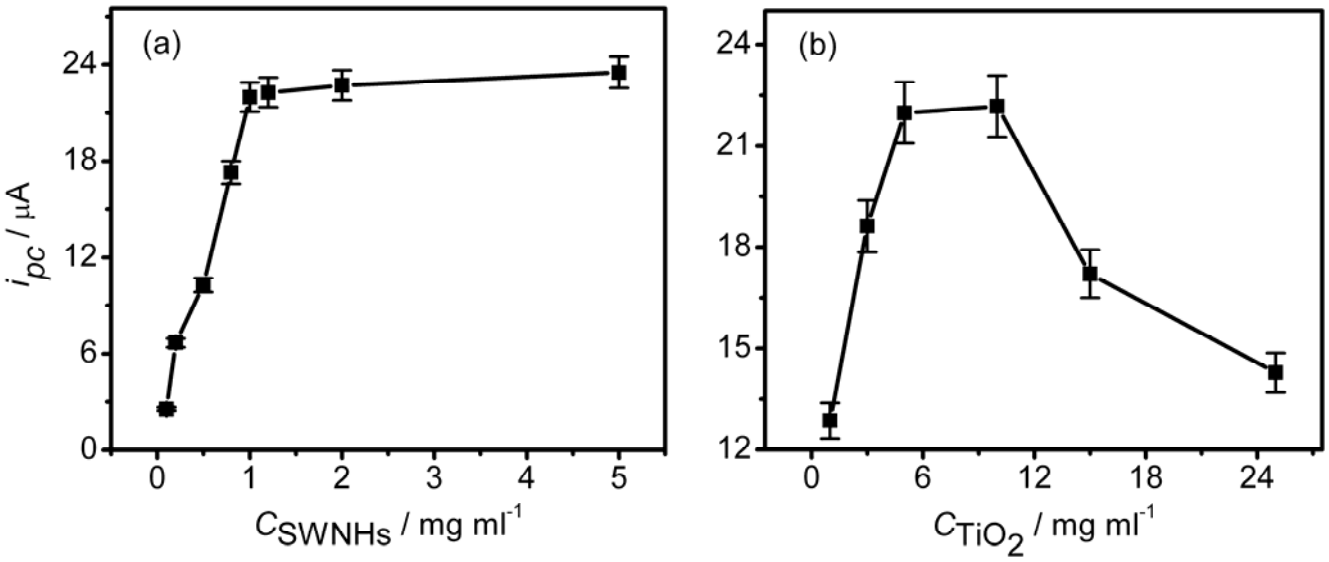

Fig. S8 Effects of SWNHs (a) and TiO_2 (b) for preparation of SWNHs-TiO_2-porphyrin nanohybrid on electrocatalytic peak current in 0.1 M PBS containing 100 μM CAP at 100 mV s^{-1}.

Amperometric response to CAP

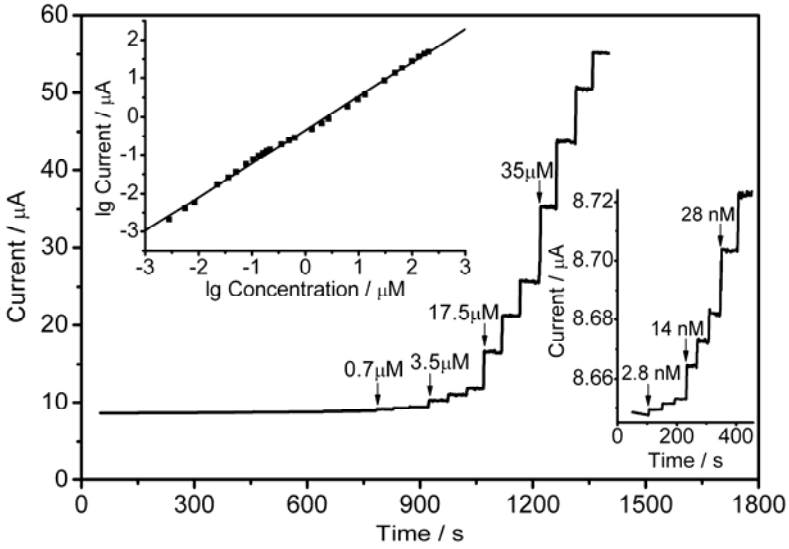

Fig. S9 Successive amperometric response of SWNHs-TiO_2-porphyrin modified GCE to CAP in 0.1 M pH 7.0 PBS at –0.56 V. Upper inset: calibration curve; lower inset: amplified response.

Stability of the sensor upon consecutive cyclic voltammetric sweep

In 0.1 M pH 7.0 PBS containing 50 μM CAP, the cyclic voltammogram of the sensor for consecutive fifty scans between 0 and -1.0 V showed acceptable stability of the sensor. The response of CAP at the fiftieth scan remained 94.1% of its initial response (Fig. S10).

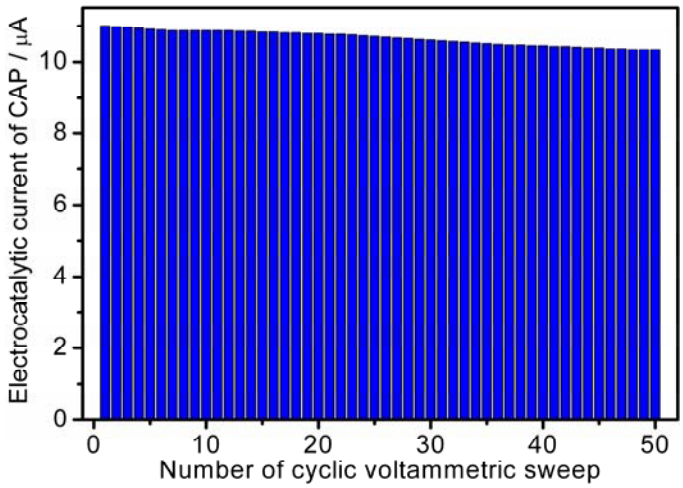

Fig. S10 Dependence of electrocatalytic peak current of 50 μM CAP at SWNHs-TiO_2-porphyrin modified GCE in 0.1 M pH 7.0 PBS on the number of cyclic voltammetric sweep at 100 mV s^{-1}.